Experimental Confirmation of the X-Ray Magnetic Circular Dichroism Sum Rules for Iron and Cobalt

C. T. Chen, Y. U. Idzerda, H.-J. Lin, N. V. Smith, G. Meigs, E. Chaban, G. H. Ho, E. Pellegrin, and F. Sette, at E. Chaban, and F. Sette,

¹AT&T Bell Laboratories, 600 Mountain Avenue, Murray Hill, New Jersey 07974

²Naval Research Laboratory, Washington, DC 20375

³Department of Physics, University of Pennsylvania, Philadelphia, Pennsylvania 19104

(Received 12 May 1994; revised manuscript received 30 September 1994)

High precision, $L_{2,3}$ -edge photoabsorption and magnetic circular dichroism spectra of iron and cobalt were measured in transmission with *in situ* grown thin films, eliminating experimental artifacts encountered by the indirect methods used in all previous measurements. The magnetic moments determined from the integrals of these spectra are found to be in excellent agreement (within 3%) for the orbital to spin moment ratios, and in good agreement (within 7%) for the individual moments, with those obtained from Einstein-de Haas gyromagnetic ratio measurements, demonstrating decisively the applicability of the individual orbital and spin sum rules.

PACS numbers: 78.70.Dm, 75.25.+z, 75.50.Bb, 75.50.Cc

Orbital and spin magnetic moments are invaluable fundamental quantities for understanding the macroscopic magnetic properties of matter. Although techniques have been successfully utilized to measure these values, their determination with element specificity remains a very difficult, but important, task. The decomposition of the total magnetic moment of a multicomponent, heteromagnetic system into the orbital and spin moment contributions of each element would be a tremendous advance in understanding the mechanisms underlying technologically important aspects of multilayer and alloy magnetic materials.

Concurrent with the x-ray magnetic circular dichroism experimental developments [1], two important magneto-optical sum rules have been derived, proposing a new procedure to deduce element-specific orbital and spin magnetic moments from x-ray absorption spectroscopy (XAS) and its associated magnetic circular dichroism (MCD) data [2,3]. Because of the significant implications of the sum rules, numerous experimental and theoretical studies, aimed at investigating their validity for itinerant magnetic systems, have been reported, but with widely different conclusions. The claimed adequacy of the sum rules varies from very good (within 5% agreement) to very poor (up to 50% discrepancy) [2–11].

This lack of a consensus can be attributed to the experimental artifacts inherent in the indirect x-ray absorption methods used in all previous works [4–9], and to the differences or incompleteness of theoretical treatments [2,3,10,11]. On the experimental side, the indirect x-ray absorption techniques, i.e., the total electron and fluorescence yield methods, are known to suffer from saturation and self-absorption effects that are very difficult to correct for [7,12]. The total electron yield method can be sensitive to the varying applied magnetic field, changing the electron detecting efficiency, or, equivalently, the sample photocurrent. The fluorescence yield method is insensitive to the applied field, but the yield is intrinsically not

proportional to the absorption cross section, because the radiative to nonradiative relative core-hole decay probability depends strongly on the symmetry and spin polarization of the XAS final states. On the theoretical side, it has been demonstrated by circularly polarized 2p resonant photoemission measurements of Ni that both the band structure effects and electron-electron correlations are needed to satisfactorily account for the observed MCD spectra [13]. However, it is extremely difficult to include both of them in a single theoretical framework.

To verify decisively the applicability of the individual orbital and spin sum rules to itinerant magnetic systems and to provide a stringent test for all first principle x-ray MCD calculations, we have measured high precision, $L_{2,3}$ -edge XAS and MCD spectra of Fe and Co by the transmission method with *in situ* grown thin films. Because it eliminates all the experimental artifacts mentioned above, the transmission method is the most reliable technique for testing the sum rules. The experiments were performed at the AT&T Bell Laboratories Dragon beam line at the National Synchrotron Light Source [14].

Soft-x-ray absorption spectra were obtained by measuring the photon flux transmitted through magnetic thin films using a soft-x-ray sensitive photodiode mounted 0.5 m behind the sample. Fe and Co thin films were grown under UHV conditions by e-beam evaporation onto 1 μ m thick semitransparent parylene, $(C_8H_8)_n$, substrates. The film thickness (50–70 Å) was chosen to keep the absorption dips of the L_3 peak in the range of (20-30)%, optimizing the signal to background ratio while preventing the loss of spectral fidelity in converting the transmission spectra into absorption cross sections. For these measurements, the photon incident angle, energy resolution, and circular polarization degree were set at 45°, 0.5 eV, and 76%, respectively. The applied magnetic field direction was along the intersection of the incidence plane and the sample surface plane. The MCD data were taken by alternating between two opposite directions of a *saturation* electromagnetic field (held at ± 500 Oe) at each photon energy. Square hysteresis loops with low coercivities (<100 Oe) were observed by *in situ* element-specific magnetic hysteresis measurements [15]. Together with our extended x-ray absorption fine structure, reflection high-energy electron diffraction, and conventional magnetometry measurements, we found that these Fe and Co thin films are of a high magnetic quality, and their structure and total magnetic moments are nearly identical to those of bulk materials.

Figure 1(a) shows the incident-photon-flux-normalized transmission XAS spectra of Fe/parylene thin films taken with the projection of the spin of incident photons parallel $(I_+, \text{ solid curve})$ and antiparallel $(I_-, \text{ dashed curve})$ to the spin of the Fe 3d majority electrons. Magnetization independent spectra of parylene substrates were also measured $(I_s, dotted curve)$ in order to calculate the relative absorption cross sections from these transmission spectra using the well-known equation, $\mu_{+}(\omega) \propto$ $-\ln[I_{\pm}(\omega)/I_{s}(\omega)]$. After taking into account the photon incident angle and the circular polarization degree, i.e., multiplying $\mu_{+}(\omega) - \mu_{-}(\omega)$ by $[1/\cos(45^{\circ})]/0.76$, while keeping $\mu_{+}(\omega) + \mu_{-}(\omega)$ the same, Figs. 1(b), 1(c), and 1(d) show, respectively, the resulting $\mu_{+}(\omega)$, $\mu_{+}(\omega)$ – $\mu_{-}(\omega)$ (the MCD spectra), and $\mu_{+}(\omega) + \mu_{-}(\omega)$ (the XAS spectra). The corresponding spectra for cobalt are shown in Fig. 2. Unlike all previous works taken with indirect x-ray absorption methods, no additional data manipulations are needed for these transmission spectra.

According to the x-ray MCD sum rules, the orbital [2] and spin [3] magnetic moments can be determined from the XAS and MCD spectra by the following equations:

$$m_{\text{orb}} = -\frac{4 \int_{L_3 + L_2} (\mu_+ - \mu_-) d\omega}{3 \int_{L_3 + L_2} (\mu_+ + \mu_-) d\omega} (10 - n_{3d}), \quad (1)$$

$$m_{\text{spin}} = -\frac{6 \int_{L_3} (\mu_+ - \mu_-) d\omega - 4 \int_{L_3 + L_2} (\mu_+ - \mu_-) d\omega}{\int_{L_3 + L_2} (\mu_+ + \mu_-) d\omega} \times (10 - n_{3d}) \left(1 + \frac{7 \langle T_z \rangle}{2 \langle S_z \rangle}\right)^{-1}, \quad (2)$$

where $m_{\rm orb}$ and $m_{\rm spin}$ are the orbital and spin magnetic moments in units of $\mu_B/{\rm atom}$, respectively, and n_{3d} is the 3_d electron occupation number of the specific transition metal atom. The L_3 and L_2 denote the integration range. $\langle T_z \rangle$ is the expectation value of the magnetic dipole operator and $\langle S_z \rangle$ is equal to half of $m_{\rm spin}$ in Hartree atomic units. In these equations, we have replaced the linear polarized spectra, $\mu_0(\omega)$, by $[\mu_+(\omega) + \mu_-(\omega)]/2$. In order to verify the individual orbit and spin sum rules, a 3d electron occupation number and a function for removing the $L_{2,3}$ absorption edge jumps are needed. However, for testing the orbital to spin relative sum rule, i.e., Eq. (1) divided by Eq. (2), this additional information is not needed and only the MCD spectra alone are required.

To assist in the evaluation of the required MCD integrals, Figs. 1(c) and 2(c) also show the integrations of the MCD spectra, starting from 20 eV below the

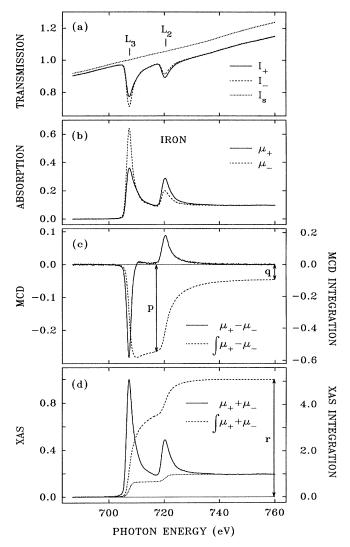


FIG. 1. $L_{2,3}$ -edge XAS and MCD spectra of iron: (a) transmission spectra of Fe/parylene thin films, and of the parylene substrates alone, taken at two opposite saturation magnetizations; (b) the XAS absorption spectra calculated from the transmission data shown in (a); (c) and (d) are the MCD and summed XAS spectra and their integrations calculated from the spectra shown in (b). The dotted line shown in (d) is the two-step-like function for edge-jump removal before the integration. The p and q shown in (c) and the r shown in (d) are the three integrals needed in the sum-rule analysis.

 L_3 white line to 40 eV above the L_2 white line. The saturation behavior near the end of the integrated spectra clearly illustrates that there is no significant MCD signal at photon energies 40 eV above the L_2 white line. The integral for the whole range, $L_3 + L_2$, can be precisely determined from the integrated spectrum, i.e., the q value shown in the figures. There is a minor uncertainty, however, for integrating the L_3 edge alone, because some of its signal may overlap with that of the L_2 edge. By choosing a cutoff at the onset of the L_2 white line, one can

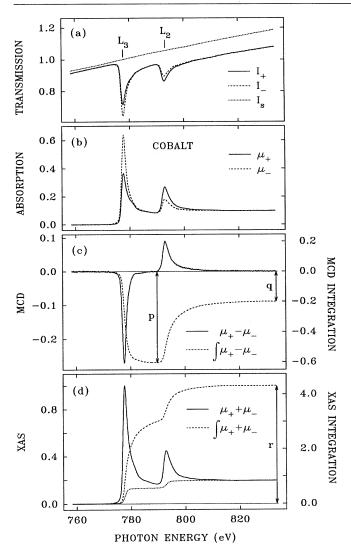


Fig. 2. $L_{2,3}$ -edge XAS and MCD spectra of cobalt. The descriptions for figures (a)–(d) are the same as those of Fig. 1.

determine the integral for the L_3 edge, i.e., the p value shown in the figures. Since the p is much larger than q, a slight uncertainty in p will not change significantly the $m_{\rm orb}$ to $m_{\rm spin}$ ratios. First-principle band structure calculations give $\langle T_z \rangle/\langle S_z \rangle$ values of -0.38% for bcc Fe, and -0.26% for hcp Co [11]. By neglecting the $\langle T_z \rangle/\langle S_z \rangle$ term in the spin sum rule, the $m_{\rm orb}$ to $m_{\rm spin}$ ratios can then be calculated as 2q/(9p-6q).

The $m_{\rm orb}$ to $m_{\rm spin}$ ratios thus determined from MCD data, those obtained by gyromagnetic ratio measurements, and the results of various theoretical calculations are listed in Table I. The MCD results are found to be in excellent agreement with those of gyromagnetic ratio measurements [16]. Of the theoretical calculations, the OP-LSDA (orbital polarization local spin density approximation) [17] are in very good agreement with the MCD and gyromagnetic ratio measurements. If the orbital polarization effect

is turned off, the result of the OP-LSDA calculation [17] is close to those of the SPR-LMTO (spin polarized relativistic linear muffin tin orbital) [10] and the FLAPW (full potential linear augmented plane wave) [11] calculations which did not include the orbital polarization effect. Our work clearly supports the theoretical notion that the inclusion of the orbital-orbital interaction is essential to completely account for the orbital magnetic moment [17].

In order to verify the applicability of the individual orbital and spin sum rules, we have adopted a simple no-free-parameter two-step-like function for removing the L_3 and L_2 edge jumps. The thresholds for the two-steplike function are set to the peak positions of the L_3 and L_2 white lines. The height of the L_3 (L_2) step was set to 2/3 (1/3) of the average intensity of the last 15 eV of the spectra, according to its quantum degeneracy, 2i + 1. Each step function was then convoluted with a Voigt function to simulate the intrinsic linewidth and experimental resolution. The two-step-like functions and the integrations of the XAS spectra, after edge-jump removal, of Fe and Co are shown in Figs. 1(d) and 2(d), respectively. The r values labeled in the figures are the XAS integrals needed in the individual sum rules, which were found to be quite insensitive to the details of the two-step-like function and the photon energy resolution [18]. For n_{3d} , we used the values of 6.61 for Fe, and 7.51 for Co, as averaged from those values reported in recent theoretical calculations [10,11]. Together with the p and q values from the MCD integration, the individual $m_{\rm orb}$ and $m_{\rm spin}$ can be calculated as $-4q(10-n_{3d})/3r$ and $-(6p - 4q)(10 - n_{3d})/r$, respectively. The values so determined, together with those from other works, are listed in Table I and show good agreement with those obtained by gyromagnetic ratio measurements. The experimental errors bars of the MCD results are estimated to be 2% for $m_{\rm orb}/m_{\rm spin}$ and 4% for $m_{\rm orb}$ and $m_{\rm spin}$.

The excellent agreement in $m_{\rm orb}/m_{\rm spin}$ between the MCD and gyromagnetic results is unexpected, considering that, unlike the gyromagnetic ratio measurements, the $L_{2,3}$ MCD of transition metals are only sensitive to the 3d component of magnetic moments, and that the $\langle T_z \rangle / \langle S_z \rangle$ term has been omitted in the above analysis. It was found from theoretical calculations that these omitted terms are very small (few %) and in opposite signs [11,17]. Using the calculated 4s/4p to 3d spin moment ratios [17] and the $\langle T_z \rangle / \langle S_z \rangle$ values mentioned above [11], the MCDdetermined spin moments need to be corrected by only -1.9% for Fe, and -3.6% for Co; no correction is necessary for the orbital moments. After including these minor corrections and using the measured ionization thresholds for the step functions [18], the corrected $m_{\rm orb}/m_{\rm spin}$ and $m_{\rm spin}$ are listed on the last line of Table I, showing excellent agreement to the gyromagnetic ratio results (within 3% for $m_{\rm orb}/m_{\rm spin}$ and 7% for $m_{\rm orb}$ and $m_{\rm spin}$). The slightly larger disagreement among the individual moments can be attributed to the discrepancies in the calculated n_{3d} [10,11], possible variations in the two-step-like function [18], or

TABLE I. Orbital and spin magnetic moments of bcc Fe and hcp Co in units of μ_B /atom.

	Fe (bcc)			Co (hcp)		
	$m_{ m orb}/m_{ m spin}$	$m_{ m orb}$	$m_{ m spin}$	$m_{\rm orb}/m_{\rm spin}$	$m_{ m orb}$	$m_{ m spin}$
MCD and sum rules	0.043	0.085	1.98	0.095	0.154	1.62
Gyromagnetic ratio [16]	0.044	0.092	2.08	0.097	0.147	1.52
OP-LSDA [17]	0.042	0.091	2.19	0.089	0.140	1.57
OP-LSDA (with OP off) [17]	0.027	0.059	2.19	0.057	0.090	1.57
SPR-LMTO [10]	0.020	0.043	2.20	0.054	0.087	1.60
FLAPW [11]	0.023	0.050	2.16	0.045	0.071	1.58
MCD and sum rules (corrected)	0.043	0.086	1.98	0.099	0.153	1.55

the uncertainties (a few %) in the circular polarization degree of the incident photons. Although the derivation of the sum rules was based on an atomic picture, it is conceivable that the core-excitonic nature of the $2p \rightarrow 3d$ transition reduces the band structure effects, making them applicable to itinerant magnetic systems. We emphasize, however, that the universal applicability of the x-ray MCD sum rules, particularly for low symmetry systems, and of the two-step-like function adopted in this work still remain to be verified, and that high precision XAS and MCD spectra, free of any experimental artifacts, as well as reliable $\langle T_z \rangle$ and n_{3d} are absolutely necessary for testing and utilizing the sum rules.

We thank D.B. McWhan, J. Stöhr, and O. Eriksson for useful discussions. The National Synchrotron Light Source is supported by the U.S. Department of Energy under Contract No. DE-AC02-76CH00016.

- *Present address: Synchrotron Radiation Research Center, Hsinchu Science-Based Industrial Park, Hsinchu 30077, Taiwan, Republic of China.
- [†]Present address: Advanced Light Source, Lawrence Berkeley Laboratory, Berkeley, CA 94720.
- [‡]Present address: European Synchrotron Radiation Facility, BP220, F-38043, Grenoble CEDEX ,France.
- See for example, G. Schütz et al., Phys. Rev. Lett. 58, 737 (1987); C. T. Chen et al., Phys. Rev. B 42, 7262 (1990);
 T. Koide et al., ibid. 44, 4697 (1991); and also Jpn. J. Appl. Phys. 32, Suppl. 32-2 (1993).
- [2] B. T. Thole, P. Carra, F. Sette, and G. van der Laan, Phys. Rev. Lett. 68, 1943 (1992).
- [3] P. Carra, B. T. Thole, M. Altarelli, and X. Wang, Phys. Rev. Lett. 70, 694 (1993).
- [4] The previous neutron form factor analyses did not provide an independent determination for the orbital to spin moment ratios, and the neutron results quoted by Ref. [3] are inappropriate for quantitative comparisons. For a discussion of the neutron results, see for example, D. B. McWhan, J. Synchrotron Rad. 1, 83 (1994).
- [5] F. Sette, C.T. Chen, Y. Ma, S. Modesti, and N.V. Smith, in X-ray Absorption Fine Structure, edited by S.S. Hasnain (Ellis Horwood, New York, 1991); C.T. Chen, N.V. Smith, and F. Sette, Phys. Rev. B 43, 6785 (1991).

- [6] Y. Wu, J. Stöhr, B.D. Hermsmeier, M.G. Samant, and D. Weller, Phys. Rev. Lett. 69, 2307 (1992).
- [7] J. Vogel and M. Sacchi, Phys. Rev. B 49, 3230 (1994).
- [8] T. Böske, W. Clemens, C. Carbone, and W. Eberhardt, Phys. Rev. B 49, 4003 (1994).
- [9] W.L. O'Brian, B.P. Tonner, G.R. Harp, and S.S.P. Parkin, J. Appl. Phys. 76, 6462 (1994); W.L. O'Brian and B.P. Tonner, Phys. Rev. B 50, 12672 (1994).
- [10] G. Y. Guo, H. Ebert, W. M. Temmerman, and P. J. Durham, in *Metallic Alloy: Experimental and Theoretical Perspectives*, edited by J. S. Faulkner (Kluwer Academic, Dordrecht, 1993); Phys. Rev. B 50, 3861 (1994).
- [11] R. Wu, D. Wang, and A. J. Freeman, Phys. Rev. Lett. 71, 3581 (1993); R. Wu and A. J. Freeman, Phys. Rev. Lett. 73, 1994 (1994).
- [12] Y. Idzerda *et al.*, Nucl. Instrum. Methods Phys. Res., Sect. A **347**, 134 (1994).
- [13] L. H. Tjeng et al., Phys. Rev. B 48, 13378 (1993).
- [14] C.T. Chen and F. Sette, Rev. Sci. Instrum. **60**, 1616 (1989); C.T. Chen, *ibid.* **63**, 1229 (1992).
- [15] C. T. Chen et al., Phys. Rev. B 48, 642 (1993).
- [16] D. Bonnenberg, K. A. Hempel, and H. P. J. Wijn, in Magnetic Properties of 3d, 4d, and 5d Elements, Alloys and Compounds, edited by K.-H. Hellwege and O. Madelung, Landolt-Bornstein, New Series (Springer-Verlag, Berlin, 1986), Vol. III/19a, p. 178, and references therein.
- [17] P. Söderlind, O. Eriksson, B. Johansson, R.C. Albers, and A. M. Boring, Phys. Rev. B **45**, 12911 (1992); O. Eriksson, B. Johansson, R.C. Albers, and A. M. Boring, *ibid.* **42**, 2707 (1990). These works showed that the 4s and 4p have no contribution to the orbital moments, but they do have small negative contributions to the spin moments. The calculated 3d, 4s, and 4p contributions to the spin moments are 2.26, -0.012, and -0.06 for bcc Fe, and 1.64, -0.014, and -0.06 for hcp Co (in units of μ_B /atom).
- [18] We found that, by using the $2p_{3/2,1/2}$ binding energies determined by XPS, i.e., 706.75 (777.90) and 719.95 (792.95) eV, for the $L_{3,2}$ ionization thresholds, the r value will change by only -1.7% (+0.7%) for Fe (Co). The average intensity of the last 10 or 20 eV of the XAS spectra was found to be within 0.5% of that of the last 15 eV. Our computer simulation shows that XAS spectra taken with 2 eV worse photon energy resolution will increase the r value by only 0.7% for Fe and 1.4% for Co, if one follows the same XAS definition of the two-step-like function mentioned in the text.